Supporting information

Glutathione-capped, renal-clearable CuS nanodots for photoacoustic imaging and photothermal therapy

Guohai Liang[†a], Xudong Jin[†a], Huan Qin [a], and Da Xing[a]**

MOE Key Laboratory of Laser Life Science & Institute of Laser Life Science, College of Biophotonics, South China Normal University, Guangzhou 510631, China.

E-mail: Liangguoh@scnu.edu.cn, E-mail: xingda@scnu.edu.cn

Table of Contents:

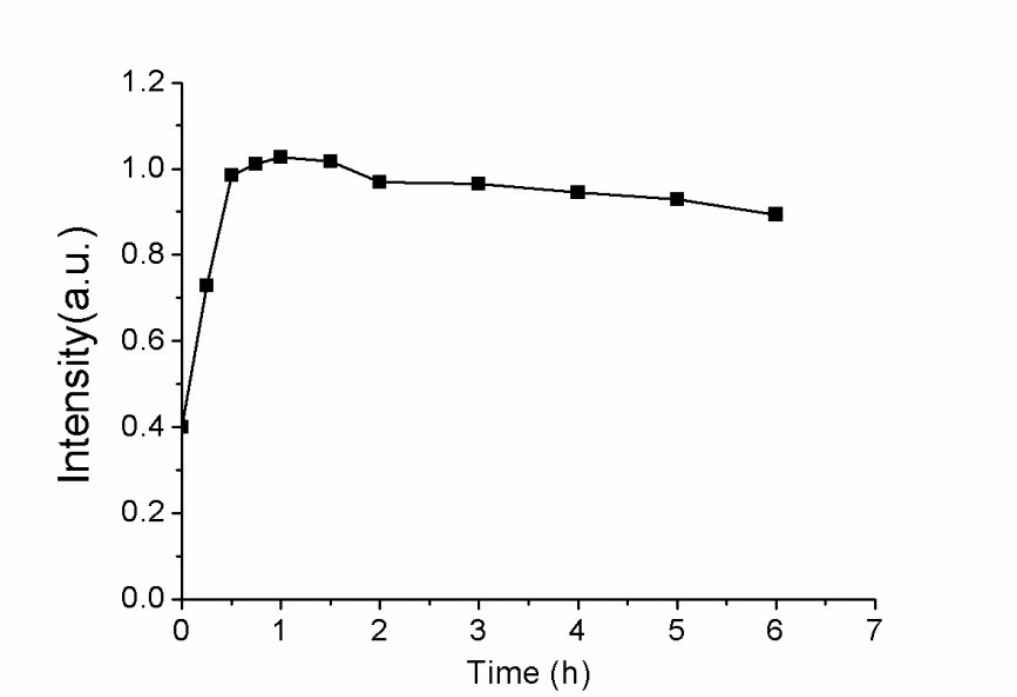

Fig. S1 Influence of reaction time on the absorption peak intensity of GSH-CuS nanodots.

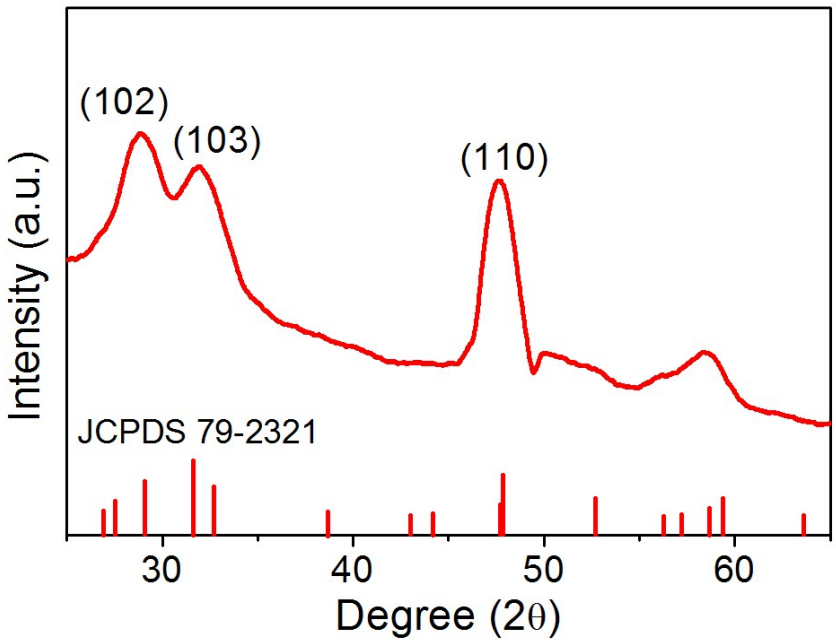

Fig. S2 XRD pattern of GSH-CuS nanodots.

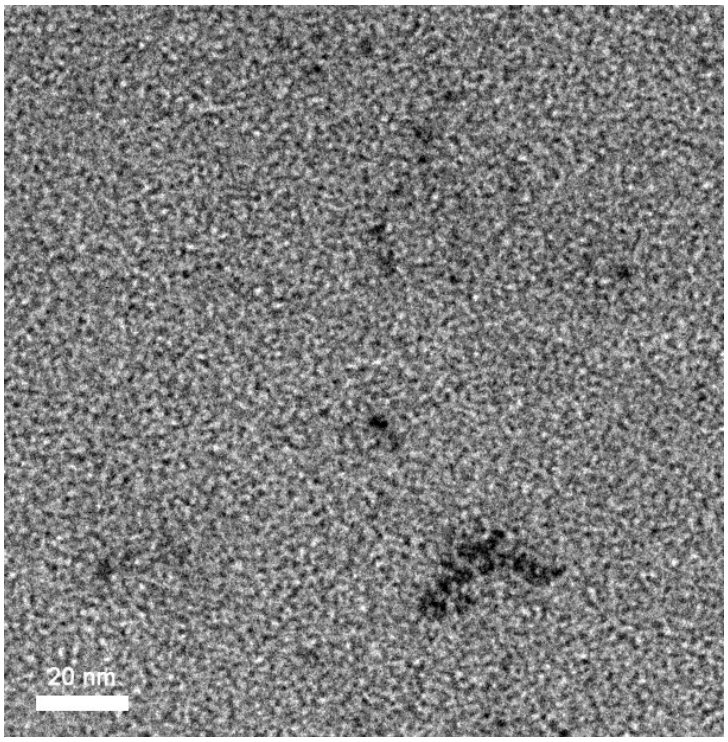

Fig. S3 TEM image of GSH-CuS nanodots acquired at the reaction time of 15 min.

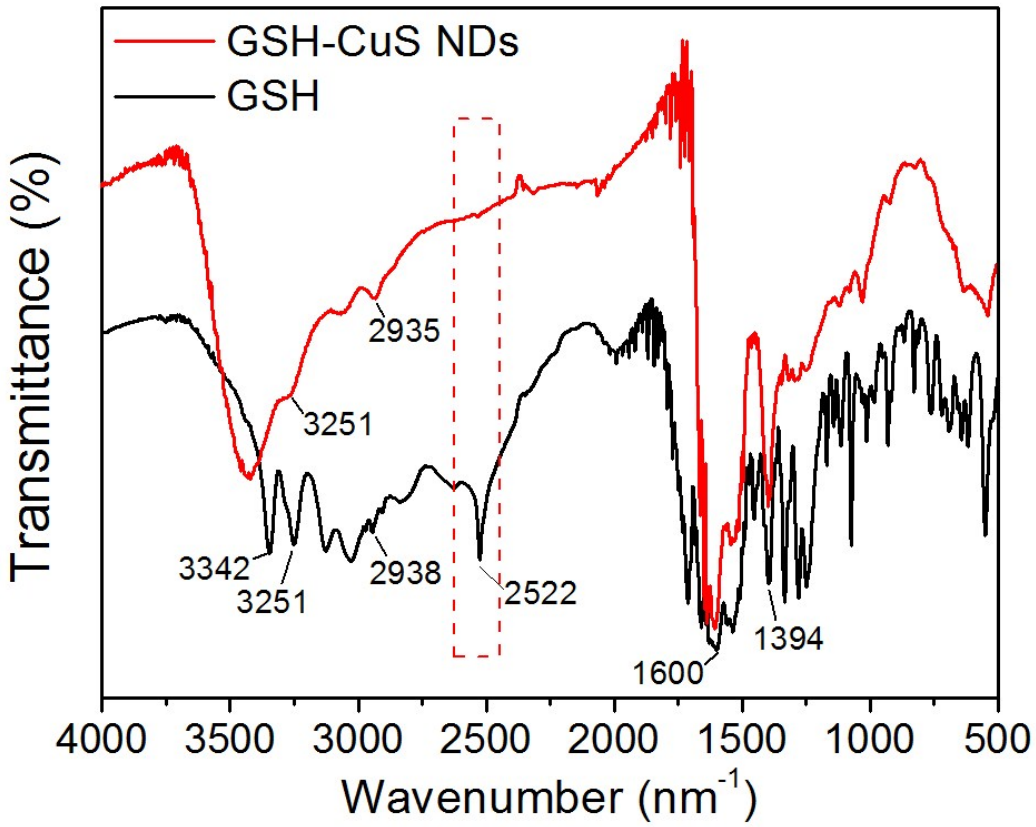

Fig. S4 FT-IR spectra of GSH and GSH-CuS NDs. The peaks at ~3251 cm^{-1}, 2935 cm^{-1} and 2522 cm^{-1} can be attributed to the stretching vibrations of N-H, C-H and S-H, respectively. The peaks at

~1600 cm^{-1} and 1394 cm^{-1} are in accordance with the vibrations of C-N and N-H band, respectively.

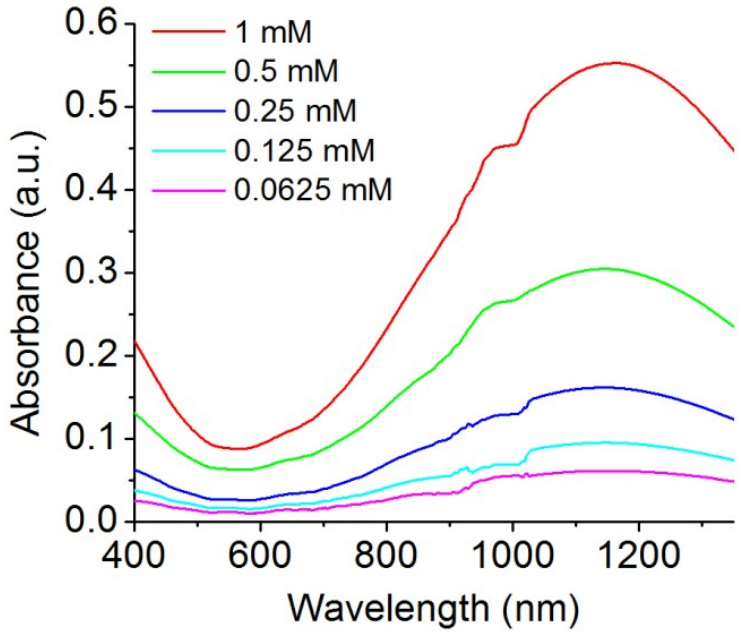

Fig. S5 UV–vis-NIR absorption spectra of aqueous solutions of GSH-CuS nanodots at varied Cu concentrations.

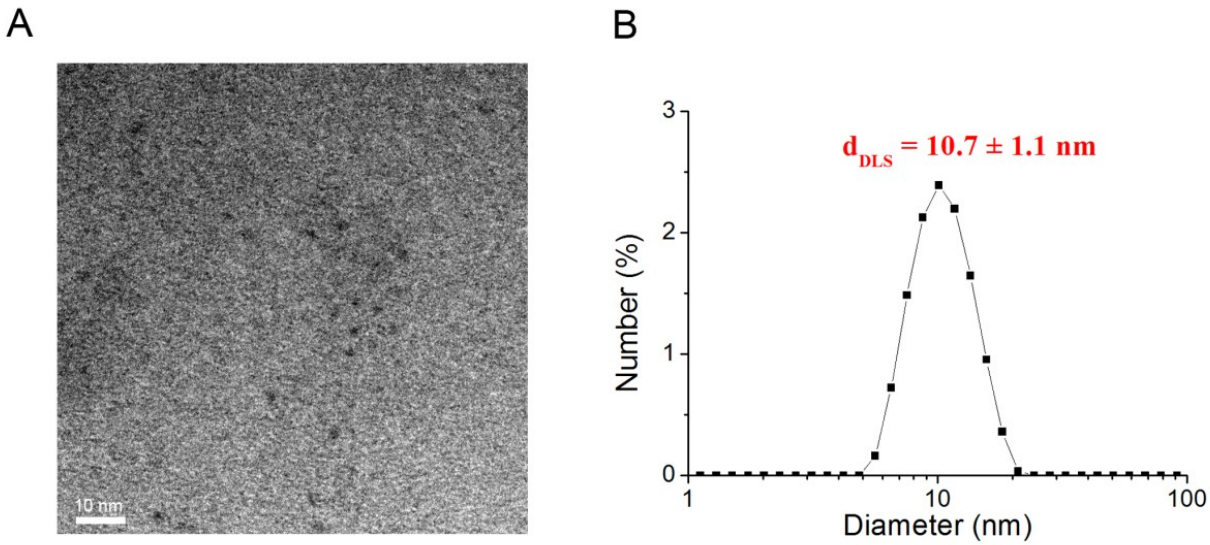

Fig. S6 TEM image (A) and hydrodynamic size analysis (B) of PVP-coated CuS nanodots.

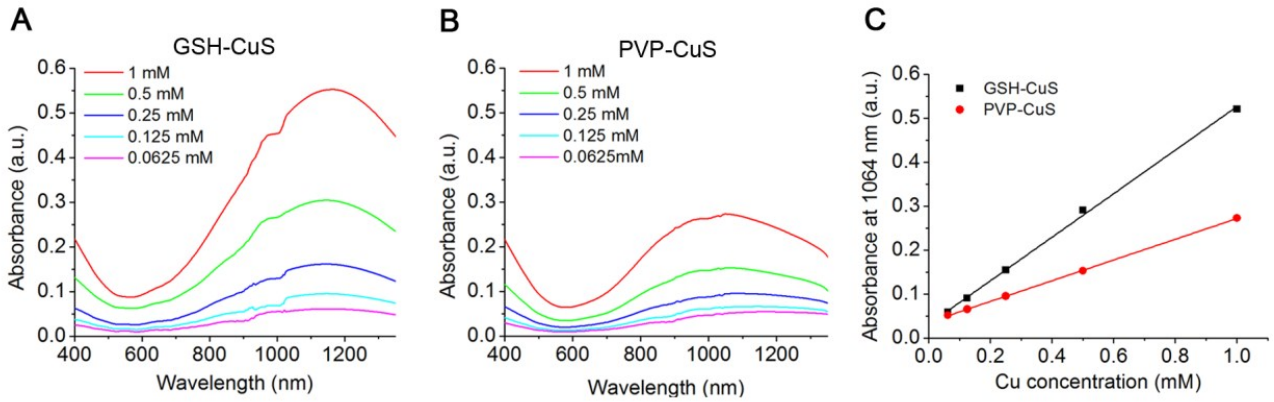

Fig. S7 Comparison of NIR absorption properties between GSH-CuS nanodots and PVP-coated CuS nanodots. (A, B) UV–vis-NIR absorption spectra of aqueous solutions of GSH-CuS nanodots (A) and PVP-coated CuS nanodots (B) at varied Cu concentrations. (C) Absorption intensities at 1064 nm of the samples.

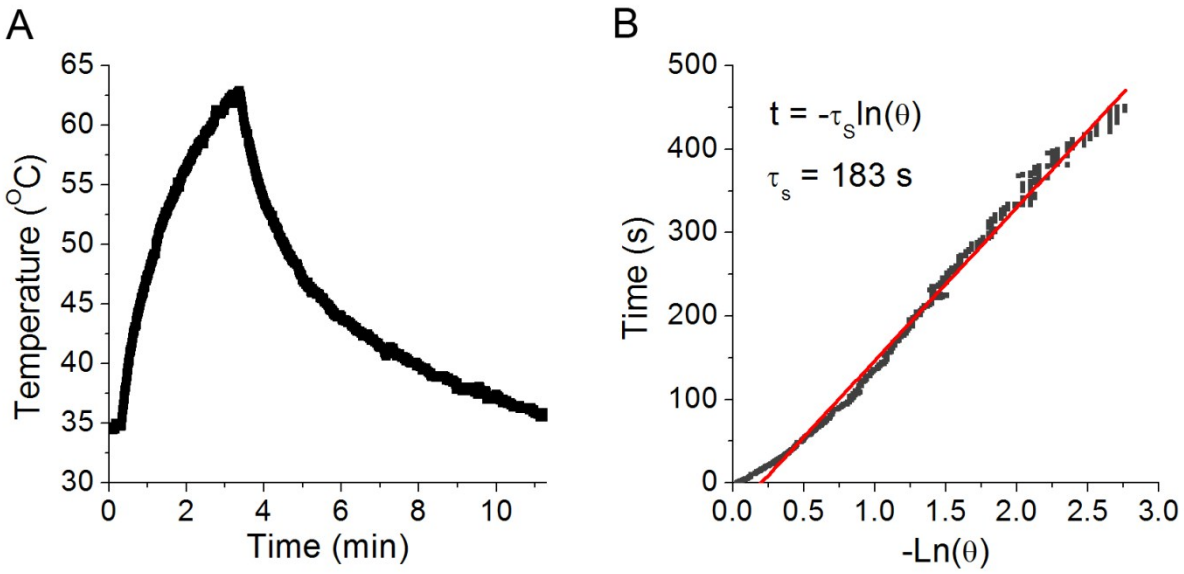

Fig. S8 Temperature evolution curves of GSH-CuS NDs in a laser on/off cycle. (A) Temperature profile of GSH-CuS NDs (0.5 mM Cu) under the irradiation of an NIR laser (980 nm, 3.0 W cm^{-2}) for 3 min and then the laser was turned off. (B) Plot of the cooling time *versus* -ln(θ) obtained from the cooling stage in (A).

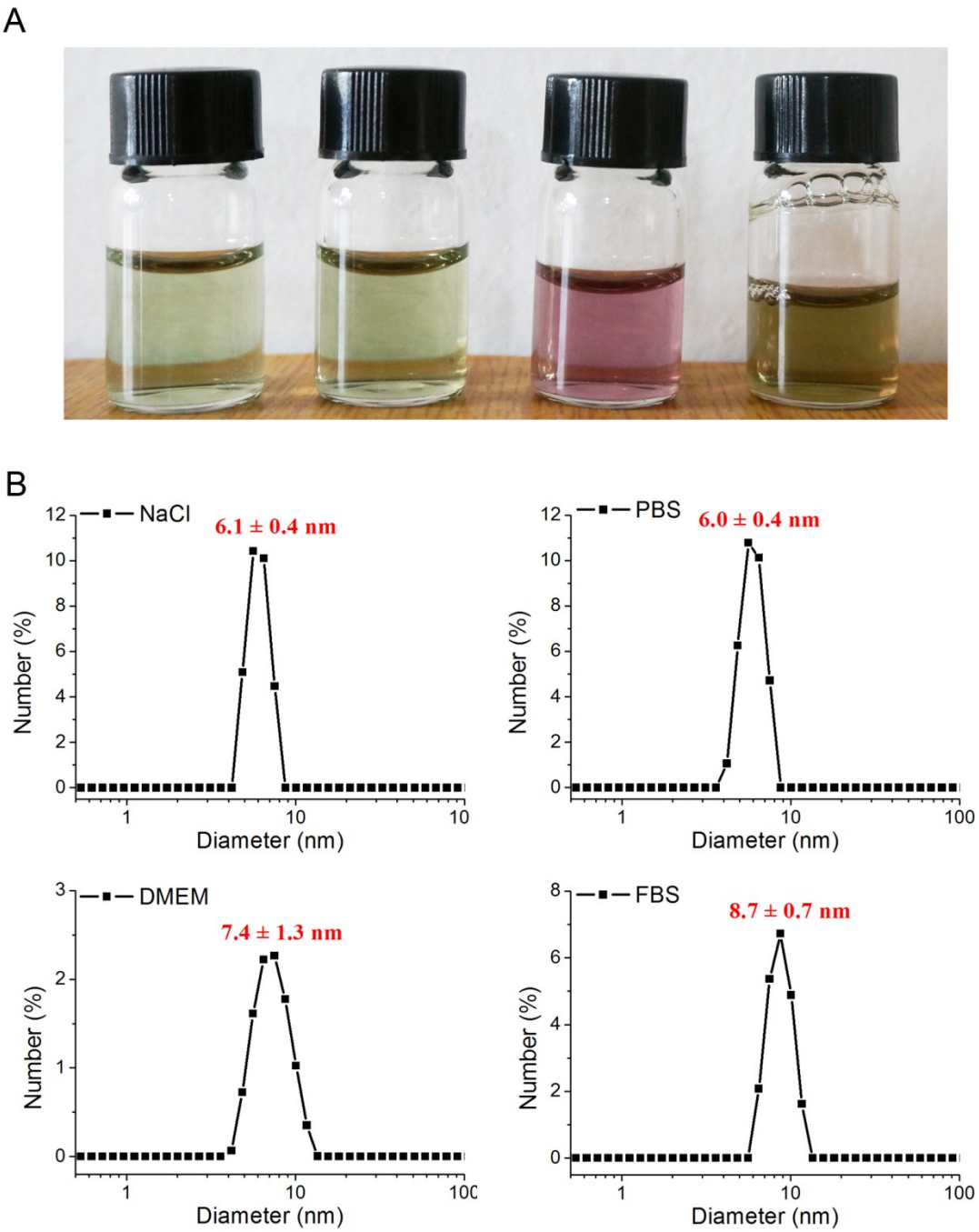

Fig. S9 Colloidal Stability of GSH-CuS NDs in different buffers. (A) Photographs of GSH-CuS nanodots in (from left to right) NaCl, PBS, 50% (v/v) Dulbecco's modified Eagle growth media (DMEM), and 25% (v/v) fetal bovine serum (FBS). (B) hydrodynamic size analysis of GSH-CuS NDs in different buffers.

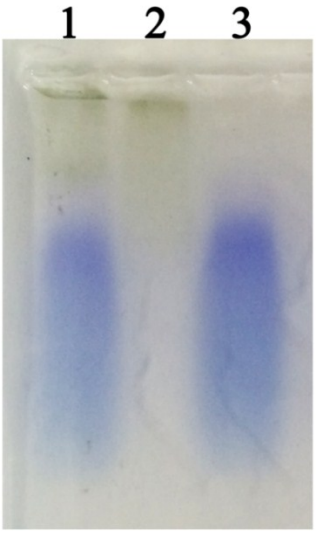

Fig. S10 Agarose gel electrophoresis of GSH-CuS nanodots with (Lane 1) or without (Lane 2) incubation with fetal bovine serum (FBS). Lane 3 was loaded with FBS alone as a control sample. The nanodots were incubated with 25% (v/v) FBS at room temperature for 1 h before loading on the gel. Serum proteins were stained by Coomassie brilliant blue 250.

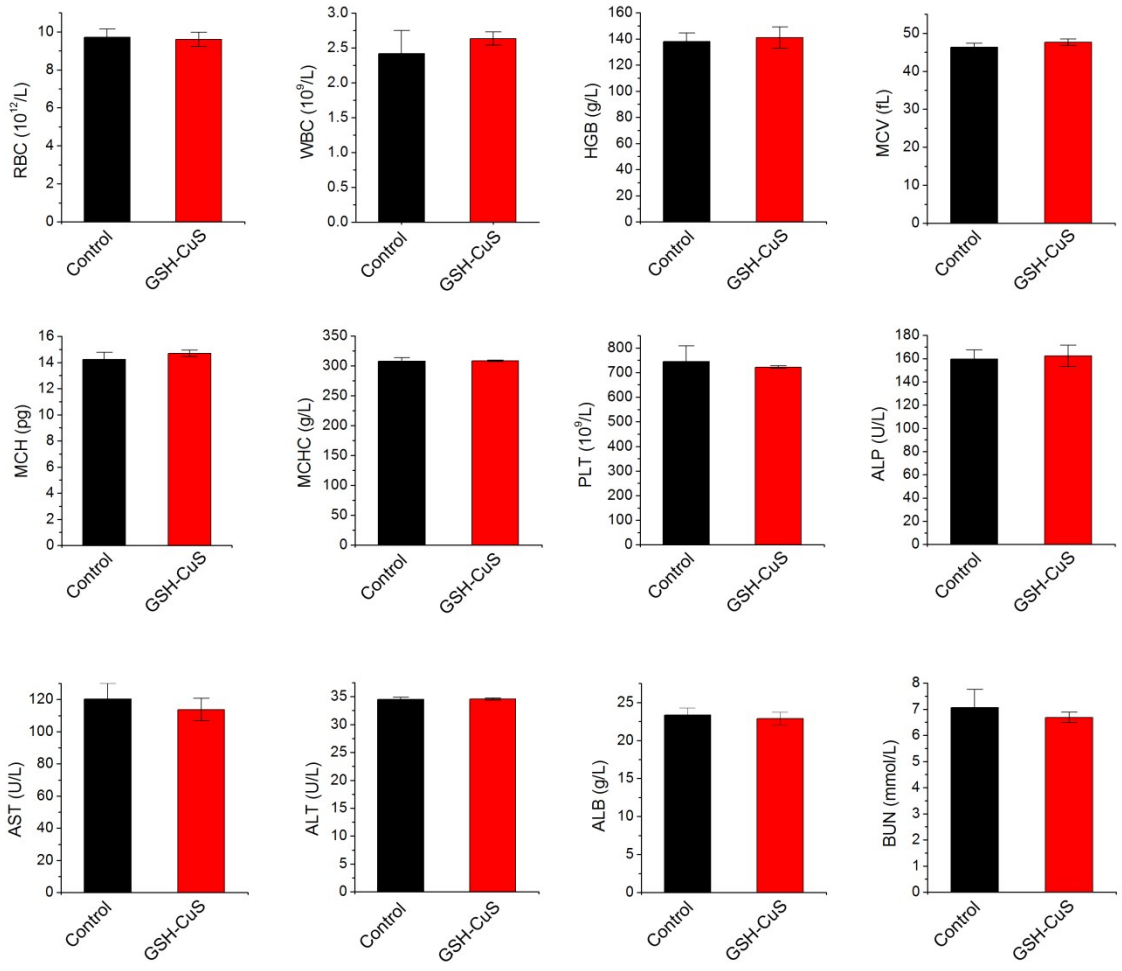

Fig. S11 Blood biochemical assay and hematology analysis.

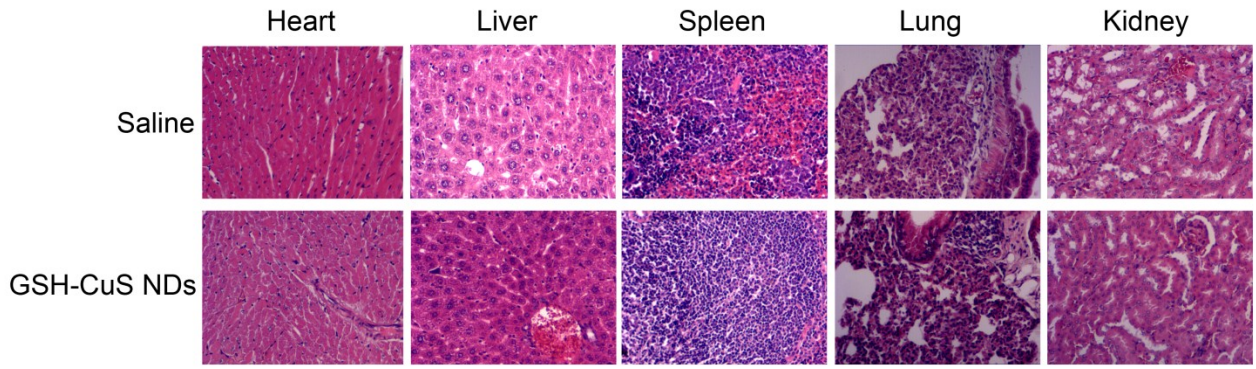

Fig. S12 Histological changes of healthy mice at 48 h after injection of saline or GSH-CuS NDs (dose =7.86 mg/kg).

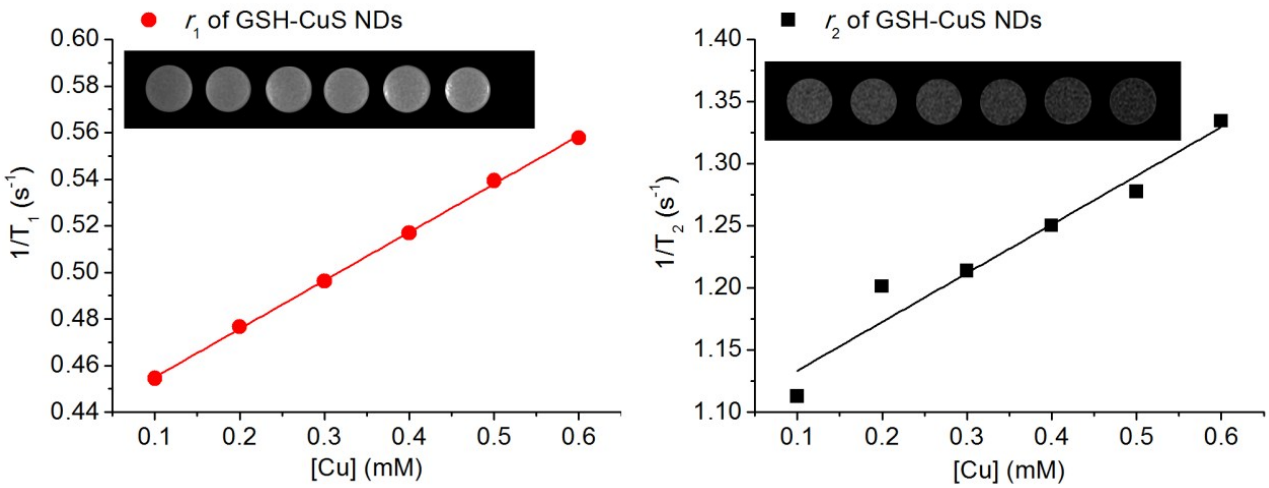

Fig. S13 Longitudinal (r_1) and transverse (r_2) relaxivity curves of GSH-CuS nanodots at 3.0 T. Samples with various Cu^{2+} concentrations (determined by ICP-AES) were used for measurements on a 3T MR scanner (TrioTim, Siemens, Germany) with a head coil at 25 °C. T_1 was measured with an IR sequence with a TR of 9000 ms, TE of 13 ms, and 10 inversion recovery points (TI = 24, 100, 200, 400, 600, 900, 1200, 2000, 3000, and 5000 ms). The acquired images had a FOV of 107 mm × 179 mm and a slice thickness of 5 mm. T_2 relaxometry was performed using a multi-echo SE sequence with a TR of 3000 ms and employing 10 TE values (27、40.5、54、67.5、81、94.5、 108 、121.5、135、148.5 ms).

Photothermal Conversion Efficiency

The photothermal conversion efficiency was determined according to the following equation (1):[1, 2]

$$\eta = \frac{hS(T_{max} - T_{amb}) - Q_{dis}}{I(1 - 10^{-A_{980}})} \quad (1)$$

Where h, S, T_{max}, T_{amb}, Q_{dis}, I, and A_{980} were the heat transfer coefficient, the surface area of the container, the equilibrium temperature, the ambient temperature, the heat dissipation from the light absorbed by the quartz sample cell, the laser power, and the absorbance of the GSH-CuS NDs at 980 nm, respectively. hS was obtained by equation (2):

$$hS = \frac{m_w C_w}{\tau_s} \quad (2)$$

Where m_w and C_w were the mass (1g) and heat capacity (4.2 J g^{-1}) of water used as the solvent, respectively. τ_s was the sample system time constant, which could be estimated from plot of the cooling time *versus* -ln(θ) shown in Fig. S8, where θ was the dimensionless driving force temperature, which could be defined as

$$\theta = \frac{(T - T_{amb})}{(T_{max} - T_{amb})} \quad (3)$$

A_{980} was determined to be 0.255 from Fig. S5 for a GSH-CuS NDs sample (0.5 mM Cu). The Q_{dis} was measured independently using a quartz cuvette cell containing pure water, and was determined to be 0.362 W. Temperature increased in this experiment from an ambient value of T_{amb} = 34.3 °C to a maximum value of T_{max} = 62.8 °C after laser irradiation, and then the laser was shut off, and the sample was allowed to cool, returning to a value of T_{amb} = 34.3 °C. Therefore the photothermal conversion efficiency of GSH-CuS NDs at 980 nm was calculated to be 21.9%.

REFERENCES

1. D. K. Roper, W. Ahn and M. Hoepfner, *J. Phys. Chem. C*, 2007, **111**, 3636-3641.
2. S.-M. Zhou, D.-K. Ma, S.-H. Zhang, W. Wang, W. Chen, S.-M. Huang and K. Yu, *Nanoscale*, 2016, **8**, 1374-1382.